# Classification of data stream in sensor network with small samples

Wei Wang[*], Min Zhang, Li Zhang

*Abstract*—**Compared with conventional narrowband radar, ultra-wideband (UWB) radar has strong anti-interference performance, low-frequency, and wide-frequency characteristics, a good penetrating ability, a high-resolution range, and a good target-recognition ability. It is effective for the detection of weak signals such as breathing or motion of the human body. Therefore, a UWB radar is widely used in the field of human body target detection for earthquake and snow disasters. At present, through-wall human target detection technology using a UWB radar has two challenging problems. First, UWB radar data has a dynamic acquisition process, whereas existing detection technologies mostly employ static learning models, resulting in an inability to process and learn data features online. There is a need to address target recognition based on sensor-network data stream. Second, UWB radar faces the problem of unbalanced data classification in the identification of through-wall targets, i.e., target recognition under small-sample conditions. To address these issues, this paper proposes an adaptive incremental recursive least-squares regression parameter estimation method based on an adaptive variable sliding window, which performs Gaussian function fitting on the data streams and adapts to the mean square error and self-adaptation variable sliding window threshold comparison to adaptively block dynamic data streams. The tensor space theory is used to extract and fuse the multi-sensor data, and the tensor depth learning algorithm is used to improve the recognition accuracy of the target detection under small-sample conditions. To evaluate the feasibility of the proposed algorithm, we use three UWB radars to build a multi-state recognition system for human targets. The data stream adaptive block effect, single and multi-sensor classification effects were tested under small-sample conditions. The experimental results indicate that the proposed algorithm not only accurately segmented the dynamic data streams but also effectively realized multi-sensor information fusion and improved the real-time target monitoring under small-sample conditions.**

*Index Terms*—**Adaptive variable sliding window, Data stream, High-order tensor space, Incremental recursive least squares, Small sample.**

## I. INTRODUCTION

THE Internet of things refers to a network of information sensing devices, such as ultra-wideband (UWB) radar sensors, infrared sensors, global positioning systems, laser scanners, and other information sensing devices [1]. It allows the connection of any item to the Internet for information exchange and communication, for realizing intelligent identification, positioning, tracking, monitoring, and management of a network [2]. Owing to its strong anti-interference ability and penetrating ability, a UWB radar is widely used in human target detection [3, 4]. In this study, a UWB radar is used to build a human target monitoring system for sensor networks.

In [5], a residual subspace projection method for through-wall human detection based on the compression sensing method was proposed, and the incomplete UWB radar data were collected for a compressed space size. In [6], kernel principal component analysis was proposed to extract the radar data, and then a support vector machine (SVM) was used to classify the four states, which achieved a good classification effect. Wu et al. [7] proposed an effective method for Time of Arrival (TOA) estimation using UWB through-wall radar, which was employed to detect and track moving targets behind the wall and verify the impact of moving target detection and tracking. Suzuli S et al. [8] applied human target detection technology for different types of walls and detected respiratory motion via the Doppler method. The singular value decomposition method was employed to reduce the clutter interference. Kumar A. and Liang Q. et al. [9] used the PulsOn220 to perform a through-wall human detection experiment on the periodic respiratory motion of a human target in a single mode, using a normalized difference matrix and a discrete Fourier transform moving-average detection technique to verify the target recognition effect for human target detection through a gypsum wall and concrete wall, respectively. Pham D. S. et al. [10] used random projection to obtain compressed data for solving the scalability challenge and directly detect abnormal targets in compressed data, thereby avoiding the problems caused by data acquisition in large sensor networks and verifying the feasibility of the anomaly detection method for real public train station datasets. In [11], by analyzing the skewness characteristics of UWB pulses modulated by life activities, a discrete short-time Fourier transform was proposed to calculate the distance from the human object to the radar antenna, which can be based on the developed set ensemble empirical mode decomposition accumulation technique to effectively counteract harmonics for estimating the frequency of human respiratory motion. The performance of the proposed method was tested in different development environments. Bugaev et al. [12] used a theoretical method and a continuous underground radar

experiment to record the spectrum of human heartbeat, respiration, and pronunciation. Liu L. and Liu Z. [13] performed UWB pulse radar experiments and used the finite-difference time-domain method to numerically simulate human cardiopulmonary respiration characteristics. The obtained data were processed using the Hilbert–Huang transform, and the respiratory characteristics of different subjects under various respiratory states were successfully identified and distinguished. In the processing of micro-Doppler features detected by human activities in [14], a three-layer deep convolutional autoencoder was proposed to initialize the weights in subsequent convolutional layers using unsupervised pre-training. It was proven that this method was not only superior to traditional classifiers but also better than deep learning models, such as the convolutional neural network and the self-encoder. In [15], a stacking denoising automatic encoder was used to detect a human target and compared with the J48 algorithm. The proposed algorithm achieved a better recognition rate for target recognition. UWB radar-based human body detection methods are becoming increasingly mature [16, 17], but most of the current models are based on static data models, and dynamic data cannot be learned in real time [18]. In addition, most human target detection classifiers are based on the overall classification accuracy, and there is always a problem of poor classification results for small-sample data [19–21].

Aiming at the problems of traditional human target detection methods under real-time data streams and small-sample conditions, this paper proposes an incremental recursive least-squares method based on an adaptive variable sliding window. The fitting parameters of the model are obtained via incremental recursive least-squares linear regression. The adaptive variable sliding window algorithm is used to segment the data streams according to the different trends of the eigenvalues. The effective data segment that is obtained improves the classification accuracy of late target recognition. At the same time, the traditional human target detection method cannot accurately identify the state of the human body under small sample conditions. Therefore, this paper proposes a high-order tensor space, which extends the sensor network data streams from the vector space to the high-order tensor space, as well as fusion and feature extraction of high-dimensional data in the high-order tensor space. The experimental results show that the tensor feature extraction algorithm based on the tensor space can not only solve the problem of high-dimensional small sample dimensions being over-high but also retain the data space–time information, so that the information between the sensor network data can be fully utilized.

This paper is organized as follows. Chapter 2 introduces the adaptive variable sliding window algorithm to realize adaptive segmentation of data streams. Chapter 3 details the representation, feature extraction, and fusion of the high-order tensor space of the sensor network data, as well as the target recognition algorithm under the small-sample condition. Chapter 4 discusses the experimental process. Chapter 5 presents the conclusion.

## II. DATA-STREAM ADAPTIVE BLOCK ALGORITHM

In the online real-time recognition process of the human body through the wall, the sensor data are continuously acquired, in the form of data streams. Therefore, the key to target recognition is determining how to adaptively acquire the data block within the data stream.

### A. Data-stream problem description

The basis of the real-time trend analysis of data streams is to divide in real-time according to a statistical characteristic index (such as the mean square error, cumulative error, or generalized likelihood ratio statistic), so that the data in the segmented data segment obey the same statistical model and the adjacent segments obey different statistical models [22–24].

For convenience, we define the one-dimensional time series data stream that arrives continuously as follows:

$$Y = \{ \upsilon_{t1}, \cdots, \upsilon_{ti}, \cdots, \upsilon_{tc}, \cdots \} \qquad (1)$$

where $t_c$ is the current moment.

Data-stream segmentation (in this study, using mean square error comparison) divides $Y$ into a series of consecutive non-empty data segments (i.e., adaptive variable sliding windows): $\{ Y_1, \cdots, Y_j, \cdots, Y_s, \cdots \}$, where the $j^{th}$ data segment is as follows:

$$Y_j = \{ \upsilon_{t_{j,1}}, \cdots, \upsilon_{t_{j,\lambda}}, \cdots, \upsilon_{t_{j,n_j}} \} \qquad (2)$$

The corresponding data arrival time is as follows:

$$t_{j,\lambda} \in \{ t_1, \cdots, t_i, \cdots, t_c, \cdots | j \in N, 1 \le j \le s; \lambda \in N, 1 \le \lambda \le n_j \} \quad (3)$$

In Equations (2) and (3), $n_j$ indicates the length of data segment $Y_j$, i.e., the length of sliding window $Y_j$, and $t_{1,1} = t_1$. The data segment $Y_s$ includes the data segment of the current data $\upsilon_{t_c}$.

Let the data in $Y_j$ be fitted with a Gaussian function:

$$Y_i = Y_{\max} \times \exp \left[ -\frac{(\upsilon_i - \upsilon_{\max})^2}{S} \right] (i = 1, 2, 3, \cdots) \quad (4)$$

Where $Y_{\max}$, $\upsilon_{\max}$, and $S$ represent the peak, peak position, and half-width information of the Gaussian function, respectively. Taking the natural logarithm on both sides of Equation (4), we obtain the following:

$$\begin{aligned} \ln Y_i &= \ln Y_{\max} - \frac{(\upsilon_i - \upsilon_{\max})^2}{S} \\ &= \left( \ln Y_{\max} - \frac{\upsilon_{\max}^2}{S} \right) + \frac{2\upsilon_i \upsilon_{\max}}{S} - \frac{\upsilon_2^i}{S} \end{aligned} \qquad (5)$$

Let $\ln Y_i = a$, $\left( \ln Y_{\max} - \frac{\upsilon_{\max}^2}{S} \right) = b_0$, $\frac{2\upsilon_{\max}}{S} = b_1$, and $-\frac{1}{S} = b_2$; then, Equation (5) is transformed into a quadratic polynomial fitting function: $a = b_0 + b_1 \upsilon_i + b_2 \upsilon_i^2$. Therefore, the estimated parameters $Y_{\max}$, $\upsilon_{\max}$, and $S$ of the Gaussian function can be transformed into a linear regression model for the quadratic polynomial function; i.e., $f(t, \theta_j) = a_j t + b_j$ is the linear regression model for the data segment $Y_j$, $\theta_j = [a_j, b_j]^T$ is the model parameter vector, the parameter

$a_j$ is the trend characteristic value of data segment $Y_j$, and $\varepsilon_j(t)$ is the independent and identically distributed zero-mean white noise. For the purpose of algorithm description, let the first data element $\upsilon_{t_{j+1,1}}$ of data segment $Y_{j+1}$ be the dividing point of $Y_j$.

The basic task of the real-time trend analysis of data streams is to perform the following calculation on the newly arrived data stream element $\upsilon_{t_c}$ based on the currently accepted data sequence $Y_{s,n} = \{\upsilon_{t_{s,1}}, \cdots, \upsilon_{t_{s,n}}\}$: 1) Split point detection (such as detecting whether $\upsilon_{t_c}$ is used as the division point of data segment $Y_{s,n}$; 2) Establish a regression model for the current data segment to calculate the current fitted model parameter values $a_j$ and $b_j$ [25-26].

### B. Incremental recursive least-squares regression modeling (IRLS)

The proposed IRLS method can correct the original model parameters with the newly arrived data and obtain new model parameters. Let the linear regression model of the current data sequence $Y_{s,n} = \{\upsilon(t_{s,1}), \cdots, \upsilon(t_{s,n})\}$ be $f(t, \theta_{s,n})$ and the data sequence be represented as $Y_{s,n} = [\upsilon(t_{s,1}), \cdots, \upsilon(t_{s,n})]^T$ in vector form. Then, $Y_{s,n} = U_{s,n} + \varepsilon_{s,n}$ among them [27]:

$$U_{s,n} = \begin{bmatrix} t_{s,1} & \cdots & t_{s,n} \\ 1 & \cdots & 1 \end{bmatrix}^T, \quad rank(U_{s,n}) = 2 < n \quad (6)$$

$\varepsilon_{s,n}$ is the expected random error vector of zero. The parameter $\theta_{s,n}$ is estimated via the least-squares method, even if $\theta_{s,n}$ is satisfied.

$$\min \mu_{s,n} \|\varepsilon_{s,n}\|^2 = \|Y_{s,n} - U_{s,n}\theta_{s,n}\|^2 \quad (7)$$

Let $p_{s,n} = U_{s,n}^T U_{s,n}, q_{s,n} = U_{s,n}^T Y_{s,n}$. Letting the derivate of $\mu_{s,n}$ be 0, the following is obtained: $\theta_{s,n} = p_{s,n}^{-1} q_{s,n}$. When the data-stream element $\upsilon(t_c)$ is reached, it is recorded as $\upsilon(t_{s,n+1})$, and the current data sequence is expanded to $Y_{s,n+1}$. Consequently, we obtain the following:

$$\begin{aligned} p_{s,n+1} &= U_{s,n+1}^T U_{s,n+1} = U_{s,n}^T U_{s,n} + U_{n+1}^T U_{n+1} \\ &= p_{s,n} + U_{n+1}^T U_{n+1} \end{aligned} \quad (8)$$

Where $U_{n+1} = [t_{s,n+1} \ 1]$. Similar to Equation (8), for $q_{s,n+1}$, we have the following:

$$q_{s,n+1} = U_{s,n+1}^T Y_{s,n+1} = q_{s,n} + U_{n+1}^T \upsilon(t_{s,n+1}) \quad (9)$$

The parameter vector of the regression model at this time satisfies the recursive equation.

$$\theta_{s,n+1} = p_{s,n+1}^{-1} q_{s,n+1} = \theta_{s,n} + p_{s,n+1}^{-1} U_{n+1}^T (\upsilon(t_{s,n+1}) - U_{n+1}\theta_{s,n}) \quad (10)$$

To avoid the inverse operation in Equation (10), the matrix inversion lemma is introduced [28].

$$[A + BCD]^{-1} = A^{-1} - A^{-1}B[DA^{-1}B + C^{-1}]^{-1}DA^{-1} \quad (11)$$

Let $A = p_{s,n}, B^T = D = U_{n+1}, C = 1, \beta_{s,n} = p_{s,n}^{-1}$, yielding the following:

$$\begin{aligned} \beta_{s,n+1} &= p_{s,n+1}^{-1} \\ &= \beta_{s,n} - (1 + U_{n+1}\beta_{s,n}U_{n+1}^T)^{-1}\beta_{s,n}U_{n+1}^T U_{n+1}\beta_{s,n} \end{aligned} \quad (12)$$

The initial value $\beta_{s,0} = \varsigma I$, $\varsigma$ is a positive number, and $I$ is a $2 \times 2$ unit matrix. When the data sequence noise is larger, $\varsigma$ takes a small value; otherwise, $\varsigma$ takes a large value. Substituting (12) into (10) yields a recursive formula for the regression model parameters: $\theta_{s,n+1} = \theta_{s,n} + \Delta\theta_{s,n}$. Where,

$$\Delta\theta_{s,n} = \beta_{s,n}U_{n+1}^T(1 + U_{n+1}\beta_{s,n}U_{n+1}^T)^{-1}(\upsilon(t_{s,n+1}) - U_{n+1}\theta_{s,n}) \quad (13)$$

Here, $(1 + U_{n+1}\beta_{s,n}U_{n+1}^T)$ is a scalar, avoiding matrix inversion. The initial value $\theta_{s,0}$ of Equation (13) is generally taken as a zero vector [29].

### C. Adaptive variable sliding window algorithm (AVSW)

This paper proposes an AVSW algorithm to segment the data sequence with a reasonable window threshold. The algorithm first sets the data segment reference window length and the longest data window length. From the starting point of the current data segment, the regression modeling is re-established for each newly arrived data stream element to improve the accuracy. When the current data segment is smaller than the reference window length, the fitting mean square error of the model is compared with the return value of the noise function $G$ to detect whether there is an abnormal point in the reference window. If the current data segment length is greater than or equal to the reference window length and the fitting mean square error of the model is greater than the preset standard segmentation point threshold, the newly arrived data are considered to be the segmentation point of the current data segment. If the current data segment length is greater than the longest data window length, the traceback starts from the starting point of the current data segment and finds a data point whose fitting mean square error is closest to the standard segmentation point threshold as the segmentation point of the current data segment [30].

The pseudo-code of the specific algorithm is shown in table1:

The reference window length $L$ is generally determined according to the waveform variation characteristics of the data stream analyzed by the applied domain.

The longest data window length $MaxLength\_Window$ is generally determined by the characteristics of the analyzed data-stream waveform changes.

The standard split point threshold $\alpha$ is generally determined by expert experience in the field of application, or multiple thresholds are selected for multiple tests to identify the most appropriate threshold.

The noise function $G(\bullet)$ is an interface function that is called when the current data segment is smaller than the reference window. It returns the split point threshold, which is determined by the specific conditions of the domain in which it is applied.

Let the mean squared variance of the model be $\mu_{s,n}$ and the

incremental recursive least-squares method be $f(\cdot)$.

TABLE I
THE PSEUDO-CODE OF THE SPECIFIC ALGORITHM

| |
|---|
| Begin |
| While ( $Y$ is not empty) |
|     // $Y$ is the dynamic data stream analyzed |
|     $\{\mu_{s,n} = f(Y_{s,n})$ |
|     // $Y_{s,n}$ is the current received data sequence, and $n$ is the length of |
|     the sequence. |
|     $If\,(n < L)$ |
|       $\{If\,(\mu_{s,n} > G(\cdot))$ |
|       $\{\upsilon_{tc}$ is the segmentation point of the data segment $Y_{s,n}$, $Y_{s,n}$'s |
|       trend eigenvalue is $\theta_{s,n} = [a_{s,n}, b_{s,n}]^T$, and the subsequent |
|       arrival data is classified into the new current data segment, and a |
|       new trend analysis is started. $\}$ |
|     $Else$  Continue to analyze the next arriving data$\}$ |
|         $If\,(n \ge L)$ |
|           $\{If\,(\mu_{s,n} > \alpha)$ |
|           $\{\upsilon_{tc}$ is the segmentation point of the data segment $Y_{s,n}$, |
|           $Y_{s,n}$'s trend eigenvalue is $\theta_{s,n} = [a_{s,n}, b_{s,n}]^T$, and |
|           the subsequent arrival data is classified into the new curr- |
|           ent data segment, and a new trend analysis is started. $\}$ |
|         $Else$   $f(n < Maxlength\_Window)$ |
|           $\{$ Continue to analyze the next arriving data $\}$ |
| $Else$   $\{While(Y_{s,n}$ is not empty$)\}$ |
|     $\{$ Search for the data point with the closest mean square error and |
|     the threshold as the segmentation point of the current data segm- |
|     ent and classify the subsequently arrived data into the new |
|     current data and start a new trend analysis. $\}$ |
| $End$ |

## III. SMALL-SAMPLE DATA PROCESSING BASED ON TENSOR SPACE

As described in this section, the tensor space is run to realize multi-sensor data fusion and feature extraction, and a tensor depth learning algorithm is proposed to realize through-wall target recognition under small-sample conditions.

To improve the accuracy of human body target recognition under small-sample conditions, multi-UWB radars are used to construct the radar sensor network for human target recognition.

Let the data streams obtained by each sensor be the length of the corresponding window obtained according to the adaptive variable sliding window algorithm as $L_1, L_2, \cdots, L_i$. The maximum value $L_{\max}$ of the data streams is the length of the experimental window. The tensor can be used to indicate that the sensor network data in the window segment is a two-dimensional matrix of size $1 \times L_{\max}$. To reduce the size and complexity of the calculation, we normalize the matrix and convert its size to $P \times Q$ (where $P$ and $Q$ are the numbers of rows and columns in the matrix, respectively). At the same time, with the UWB radars in the experiment of $N$, a third-order tensor $A^{P \times Q \times N}$ is formed as a sample.

Considering the problem that the multi-sensor RF is reflected by various obstacles, data interference occurs during transmission [31]. The tensor decomposition includes Tucker decomposition [32] and CP decomposition [33-34], and the tensor Tucker decomposition is used to process the tensor data of the sensor network [35-40]. The decomposition process is based on formula (14):

$$
\begin{aligned}
A &= \left\{ B; U^{(1)}, U^{(2)}, \cdots, U^{(N)} \right\} \\
&= B \times_1 U^{(1)} \times_2 U^{(2)} \times_3 \cdots \times_N U^{(N)} \\
&= \sum_{k_1=1}^{n_1} \sum_{k_2=1}^{n_2} \cdots \sum_{k_N}^{n_N} B_{k_1 k_2 \cdots k_N} U_{k_1}^{(1)} \otimes U_{k_2}^{(2)} \otimes \cdots \otimes U_{k_N}^{(N)}
\end{aligned}
\tag{14}
$$

Because a high dimension influences on the complexity of the classification algorithm, the eigenvalues of the obtained core tensor $B^{J \times K \times N}$ are extracted. The extraction process is the core tensor obtained for each sample, and the eigenvalues corresponding to the $N$ tangent planes are arranged in columns to form a new second-order tensor sample with a size of $C^{J \times N}$, which is the eigenvalue matrix after multi-sensor fusion.

According to the acquired multi-sensor fusion feature matrix, the tensor deep learning (TDL) model is used for multi-state classification to overcome the influence of the small-sample conditions on the classification accuracy. The algorithm process is shown in Fig. 1.
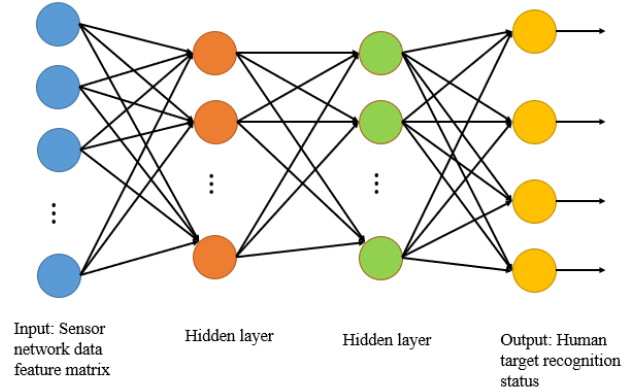


Fig. 1. TDL classification model.

## IV. EXPERIMENTAL SETUP AND ANALYSIS

To evaluate the effectiveness of the proposed algorithm, we built a three-sensor human body wall target recognition system, as shown in Fig. 2. In this experiment, the server has eight cores and 40 threads, the central processing unit is Intel Xeon E5-2620, the main frequency is 2.2 GHz, and the memory capacity is 64 GB. The algorithm runs on MATLABR2017 and is based on the deep learning framework of PyTorch.

Fig. 2. Sensor network consisting of three UWB radar devices.

## A. Experimental setup and data acquisition

The three sensors used in this paper were P410UWB devices that consisted of a transmitting antenna and a receiving antenna. The frequency range of the device was 3.1–5.3 GHz, the center frequency was 4.3 GHz, and the sampling interval was 61.024 ps. The module of P410MRM is shown in Fig. 3.

The human body target recognition experiment is a brick wall in an indoor environment. The radar module is 60 cm away from the wall, its height from the ground is 115 cm, the wall thickness is 24 cm, and all the human targets are 120 cm away from the wall, behind the wall, and facing the radar equipment. In the experiment, the static sensor network training data and the dynamic sensor network test data stream were collected in the following states: the unmanned state, the two-person quiescent state, the one-person rapid breathing state, and the two-person waving arm state. For the dynamic sensor network test data stream in an environment with an experimental length of 20 m, the car collects data in real-time at a speed of 1 m per minute.



Fig.3 Radar Model: P410MRM.

## B. Dynamic sensor network test data stream adaptive block performance

The regression parameters were modeled separately for each sensor device using the incremental recursive least-squares method, and the fitting error was compared with the adaptive

variable sliding window algorithm threshold to divide the data block for the human target recognition algorithm. Under the aforementioned conditions, the parameters of each algorithm were optimized as much as possible. Considering the waveform characteristics of the UWB radar, we set the following: the reference window length was $L = 500T$ ($T$ is the period of the UWB curve waveform), the longest data window length was $MaxLength\_Window = Lk$ ($k$ is a variable parameter, $1.5 \leq k \leq 2$, the initial value is 1.5), and the standard segmentation point threshold was $\varsigma = r \left( r \in N, 2 \leq r \leq 10 \right)$.

The experimental results are shown in Figs. 4 to 6, where the x-label represents the number of data points that is generated based on a time series and the unit is ns. But the y-label represents the pulse value corresponding to the number of each data point and has no unit. We take the fitting result graph (Fig. 4) obtained by the first sensor as an example for detailed explanation. The upper part of Fig. 4 presents the raw data, and the lower part presents the fitting data obtained via the incremental recursive least-squares method. It can be clearly seen that the algorithm can better approximate the original data, so that the fitting error is relatively small, and the fitting parameters are more accurate. The segmentation point can be better detected when the fitting error is compared with the adaptive sliding window threshold. The black parameter points in Fig. 4 are the divided segment values. They indicate that the data-stream segmentation effect is better, and the sensors have similar meanings.

We adaptively blocked the test data streams in the dynamic sensor network and input the obtained data block into the trained classification model of the training data set. The final classification result shows that the proposed adaptive block algorithm can fit the raw data to accurately identify the various human states.
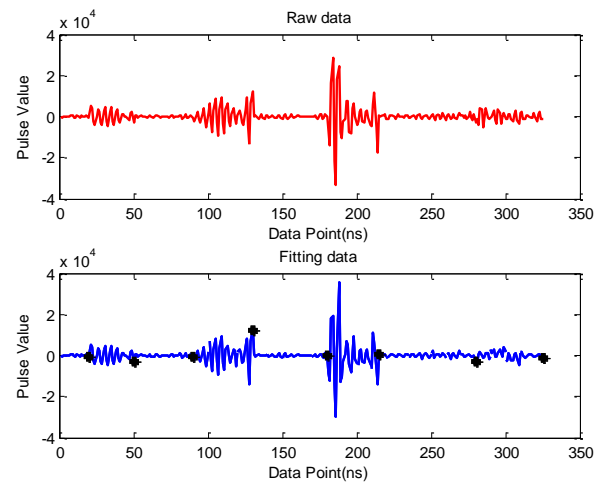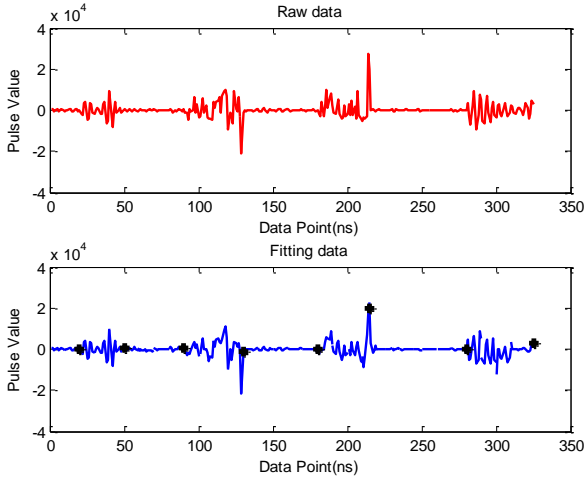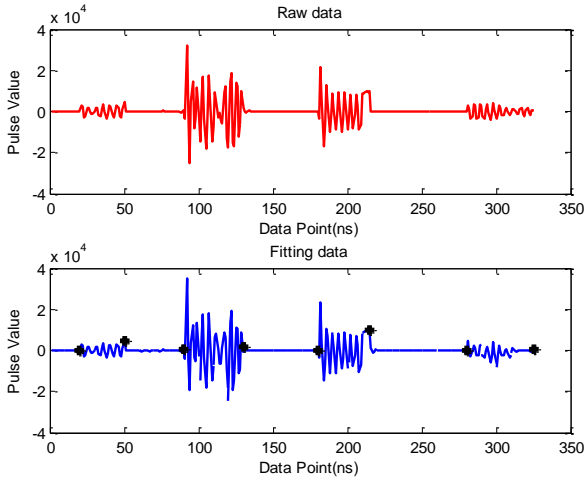


Fig.4 First sensor.

Fig.5 Second sensor.



Fig.6 Third sensor.

*C. Performance analysis of classification algorithm for sensor network data under small-sample conditions*

In this paper, the data acquired by the three sensors constitute a third-order tensor $A^{P \times Q \times 3}$, where $P$ and $Q$ represent the periodic signal domain of the sensor, i.e., the number of samples selected by each sensor and the dimensions of each sample. For the data of the training samples, we selected a periodic signal of $1 \times 900$ dimensions for each sensor, normalized the data it represents, and then transformed it into a $30 \times 30$ two-dimensional matrix. At the same time, with three UWB radar sensors, a third-order tensor with a sample size of $A^{30 \times 30 \times 3}$ was formed. Considering that the fused data contained redundant information and noise interference, we extracted the tensor features of the training data in the tensor space to obtain a core tensor of $B^{10 \times 10 \times 3}$ and obtain the corresponding tangential plane of each sample. The eigenvalues, arranged in columns, formed a new second-order tensor sample with a size of $10 \times 3$. Among them, the total number of training samples was 80, the number of positive samples unmanned was 50, the number of negative samples for two people was still 5, one person rushing to breathe was 10, and two people swinging their arms was 15. The core tensor $B^{10 \times 10 \times 3}$ obtained from each sample is input into the TDL classification algorithm for training, and the trained parameters were used during the testing of the test sample to obtain the final recognition result.

The test data used in this paper were based on the adaptive segmentation of the dynamic sensor network data stream. There was a total of nine groups (nine sets of dynamic data stream data were obtained according to the same experimental environment, and the same model parameters were used in the data segment adaptive block model); thus, the number of test samples in this study was 36, of which the number of samples with the positive unmanned state was 9, the number of samples with two people was still 9, the number of samples with one person rushing to breathe was 9, and the number of samples with two people swinging their arms was 9. The dynamic data stream was adaptively partitioned according to the time series to obtain $1 \times L_{max}$ dimension data, where $L_{max}$ is the maximum window length of the adaptive partition, i.e., the dimension of the state. To use the trained classification model for testing, we performed tensor feature extraction on the obtained test samples to obtain a third-order tensor of the same dimension as the training sample.

The third-order tensor of the test sample is represented as $Y^{10 \times 10 \times 3}$, and the number of samples was 36. It is input into the trained TDL model to compare the recognition rate of the target with the SVM. All experiments were run five times, and the average results for the five experiments are presented in Table 1. According to the same classification algorithm, i.e., vertical comparison, the fusion data using the three sensors had the highest recognition rate. The single sensor (feature extraction using principal component analysis) had a poor recognition rate, because when a single sensor collects weak signal data such as human breathing, there may be a missing part of the data, or when a single sensor encounters a fault and cannot work, this may result in a lack of data, making the measured data incomplete, which results in the final recognition effect being less than ideal. On the other hand, with the three sensors, it is possible to obtain complementary data, collect a relatively complete human target signal, and subsequently obtain a relatively high recognition effect. The horizontal comparison shows that the TDL model obtains a higher recognition rate than the SVM. This is because TDL is based on the tensor space, whereas the SVM is based on the vector space. Processing data in tensor space can preserve the connection between data, so that the feature information of the data under the small-sample condition can reflect the original data information to the greatest extent.

TABLE 2
RECOGNITION RATE OF DIFFERENT SENSORS IN DIFFERENT CLASSIFICATION ALGORITHMS

| Number of sensors | TDL | SVM |
|---|---|---|
| Sensor1 | 75.46% | 68.74% |
| Sensor2 | 75.66% | 67.56% |
| Sensor3 | 75.9% | 69.34% |
| All sensors | 91.62% | 83.54% |

Fig. 7 shows the recognition effect of each experiment in the five experiments of TDL operation. It can be seen that the proposed algorithm not only processed the dynamic data stream in real time, but also preserved the original data information to reduce the dimensionality of the high-dimensional small-sample data.
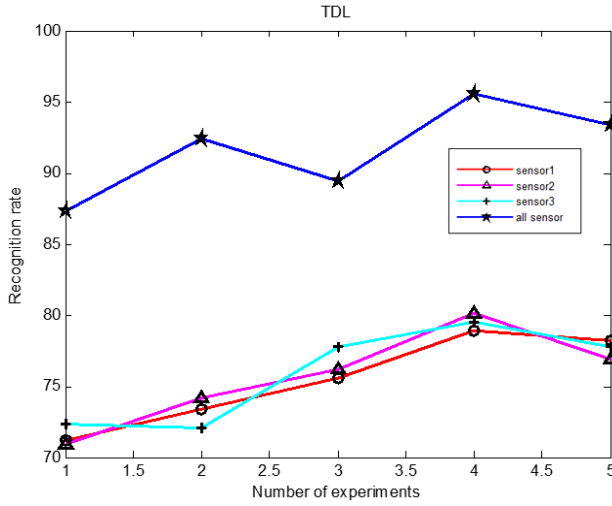
Fig. 7.  Five experimental results of TDL.



Fig. 8.  Comparison of window selection algorithms.

*D. Comparison of adaptive variable sliding window and fixed sliding window target recognition*

We compared not only the test data obtained by using the adaptive block with the trained classification model but also the sliding window length selection, which fully verifies the superiority of the proposed algorithm. In this study, the human target states were as follows: unmanned, two people are still, one person is rushing to breathe, and two people with swinging arms, which were represented by 1, 2, 3, and 4, respectively. For each data-segment length obtained in section C through the adaptive sliding window, we took the average length of each data segment as the length of the fixed window of this section, and the distance of each fixed sliding window length is equal to the fixed window length, ensuring that there is no overlap between the data obtained by the fixed window length block.

We input the data segments obtained by dividing the two window lengths into the dynamic data stream into the TDL classification model for target recognition. In the TDL target recognition, we believe that the state is within 5% of the state before and after the fluctuation of the state. Fig. 8 shows the recognition effect of the adaptive variable sliding window and the fixed window, where the x-axis represents the number of data points and the y-axis represents the data value corresponding to the number of each data point. The original data state comparison of the three sensors in the first part showed that the adaptive variable sliding window (the middle portion of Fig. 8) substantially conformed to the original target recognition. However, in the fixed window length (the last one of Fig. 8), the obtained state was misclassified, which worsened the target recognition effect, and the human target could not be recognized. In summary, the proposed algorithm can better segment the dynamic data streams and effectively identify various human targets.
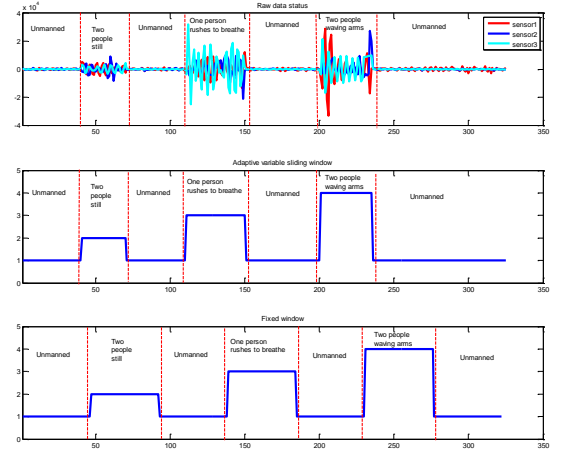
## V.  DISCUSSION AND CONCLUSION

According to the traditional algorithm for the problem of dynamic data streams and data processing under small-sample conditions, this paper proposes an incremental recursive least-squares method and an adaptive variable sliding window algorithm to adaptively segment the dynamic data stream to obtain data blocks. The data processing includes feature fusion and feature extraction algorithm based on the tensor space and builds a three-sensor human body through-wall target recognition system. In the experiment, we use the core data features obtained by the fusion of three sensors to be trained in the TDL model and SVM classification algorithms, and the test data segments obtained via adaptive segmentation are placed in the trained model to obtain the final classification result. The results indicate that the classification algorithm based on TDL can obtain up to 91.62% classification accuracy, compared with 83.54% for the SVM. Therefore, the proposed algorithm can effectively overcome the limitations of small-sample conditions and achieve high-precision real-time monitoring of human body wall penetration targets. However, the human target state setting in this paper was not comprehensive. More human body state targets and more complicated wall materials should be considered in future experiments.

## REFERENCES

[1]  G Gennarelli, G Vivone, P Braca, "Multiple Extended Target Tracking for Through-Wall Radars." IEEE Trans. Geosci. Remote Sens. **53**(12), 6482–6494 (2015).
[2]  Choi J W, Quan X, Cho S H, "Bi-Directional Passing People Counting System based on IR-UWB Radar Sensors." IEEE Internet of Things Journal, 2017, PP(99):1-1.

[3] Jia Min, Yin Zhisheng, Guo Qing, Liu Gongliang, Gu Xuemai, "Downlink Design for Spectrum Efficient IoT Network." IEEE Internet of Things Journal. 2017, PP(99): 1-8.

[4] He Feng, "Research on key technologies of human target detection and feature extraction for wideband/ultra-wideband radar motion." National University of Defense Technology, 2011.

[5] Wang W, Wang D, Jiang Y, "Multiple statuses of through-wall human being detection based on compressed UWB radar data." Eurasip Journal on Wireless Communications & Networking, 2016, 2016(1):203.

[6] Wang W, Zhang M, Wang D, et al, "Kernel PCA feature extraction and the SVM classification algorithm for multiple-status, through-wall, human being detection." Eurasip Journal on Wireless Communications & Networking, 2017, 2017(1):151.

[7] Wu S, Fang G, "Detection and Tracking of Moving Target behind Wall Using UWB Through-wall Radar." International Conference on Intelligent System Design and Engineering Application. IEEE, 2010:605-608.

[8] Suzuki S, "Sense through wall human detection using UWB radar." Eurasip Journal on Wireless Communications & Networking, 2011, 2011(1):20.

[9] Kumar A, Liang Q, Li Z, et al, "Experimental study of through-wall human being detection using ultra-wideband (UWB) radar." 2012.

[10] Pham D S, Venkatesh S, Lazarescu M, et al, "Anomaly detection in large-scale data stream networks." Data Mining & Knowledge Discovery, 2014, 28(1):págs. 145-189.

[11] Liang X, Lv T, Zhang H, et al, "`Through-wall human being detection using UWB impulse radar." Eurasip Journal on Wireless Communications & Networking, 2018, 2018(1):46.

[12] Bugaev A S, Chapursky V V, Ivashov S I, et al, "Through wall sensing of human breathing and heart beating by monochromatic radar." Tenth International Conference on Ground Penetrating Radar. IEEE, 2004:291-294.

[13] Liu L, Liu Z, Barrowes B E, "Through-Wall Bio-Radiolocation With UWB Impulse Radar: Observation, Simulation and Signal Extraction." IEEE Journal of Selected Topics in Applied Earth Observations & Remote Sensing, 2011, 4(4):791-798.

[14] Seyfioğlu M S, Özbayğglu A M, Gurbuz S Z, "Deep Convolutional Autoencoder for Radar-Based Classification of Similar Aided and Unaided Human Activities." IEEE Transactions on Aerospace & Electronic Systems, 2018, PP(99):1-1.

[15] Wang W, Jiang Y, Wang D, "Through Wall Human Being Detection Based on Stacked Denoising Auto-encoder Algorithm." International Conference in Communications, Signal Processing, and Systems. Springer, Singapore, 2017:2205-2212.

[16] Kocur D, Svecovã M, Rovåà k J, "Through-the-wall localization of a moving target by two independents ultra-wideband (UWB) radar systems." Sensors, 2013, 13(9):11969-97.

[17] Nanzer J A, "A Review of Microwave Wireless Techniques for Human Presence Detection and Classification." IEEE Transactions on Microwave Theory & Techniques, 2017, 65(5):1780-1794.

[18] Wang Chengliang, Pang Wei, Lu Zhijian, et al, "Data stream classification based on dynamic feature extraction and neural network." Computer Application, 2010, 30(6): 1539-1542.

[19] Xinmin Tao, Siyuan Hao, Dongxue Zhang et al, "Overview of classification algorithms for unbalanced data." Journal of Chongqing University of Posts and Telecommunications (Natural Science Edition), 2013, 25(1):101-110.

[20] Zhang J, Mani I, "kNN Approach to Unbalanced Data Distributions: A Case Study involving Information Extraction." In Proceedings of the ICML 2003 Workshop on Learning from Imbalanced Datasets. 2003.

[21] Padmaja T M, Dhulipalla N, Bapi R S, et al, "Unbalanced data classification using extreme outlier elimination and sampling techniques for fraud detection." International Conference on Advanced Computing and Communications. IEEE, 2007:511-516.

[22] Koski A, Juhola M, Meriste M, "Syntactic recognition of ECG signals by attributed finite automata." Pattern Recognition,1995,28(12):1927-1940.

[23] Shatkay H, Zdonik S, "Approximate queries and representations for large data sequences." Proceedings of 12th IEEE International conference on data engineering. Washington: IEEE computer society,1996:546-553.

[24] Keogh E, Chu S, Hart D, et al, "Segmenting time series: A survey and novel approach." Proceedings of IEEE International conference on data mining. Los Jose: IEEE computer society, 2001:289-296.

[25] Sylvie C, Carlos G B, Cathering C, et al, "Trends extraction and analysis for complex system monitoring and decision support." Engineering applications of artificial intelligence,2005,18(1):21-36.

[26] Zhou Wei, Wu Tiejun, "A Real-Time Trend Analysis Algorithm for Dynamic Data Flow." Control and Decision, 2008, 23(10): 1182-1185.

[27] Zhou Q, Cluett W, "Recursive identification of time-varying systems via incremental estimation." Automatica,1996,32(10):1427-1431.

[28] Petrá I, Bednárová D, "Total Least Squares Approach to Modeling: A Matlab Toolbox." Acta Montanistica Slovaca, 2010, 15(2).

[29] G, Liu H, Tong L, et al, "A least-squares approach to blind channel identification." IEEE Transactions on Signal Processing, 1995, 43(12):2982-2993.

[30] Belyaev E, Gilmutdinov M, Turlikov A, "Binary Arithmetic Coding System with Adaptive Probability Estimation by "Virtual Sliding Window." IEEE Tenth International Symposium on Consumer Electronics. IEEE, 2006:1-5.

[31] Jia Min, Liu Xin, Gu Xuemai, Guo Qing, "Joint cooperative spectrum sensing and channel selection optimization for satellite communication systems based on cognitive radio." International Journal of Satellite Communications and Networking. 2017. 35(2): 139-150.

[32] Eeghem F V, Sørensen M, Lathauwer L D, "Tensor Decompositions With Several Block-Hankel Factors and Application in Blind System Identification." IEEE Transactions on Signal Processing, 2017, 65(15):4090-4101.

[33] Veganzones M A, Cohen J E, Farias R C, et al, "Nonnegative Tensor CP Decomposition of Hyperspectral Data." IEEE Transactions on Geoscience & Remote Sensing, 2016, 54(5):2577-2588.

[34] Goulart J H D M, Boizard M, Boyer R, et al, "Tensor CP Decomposition With Structured Factor Matrices: Algorithms and Performance." IEEE Journal of Selected Topics in Signal Processing, 2016, 10(4):757-769.

[35] Tan V, Tran D, Ma W, "Tensor decomposition and application in image classification with histogram of oriented gradients." Neurocomputing, 2015, 165(C):38-45.

[36] Tan V, Tran D, Ma W, "Tensor decomposition and application in image classification with histogram of oriented gradients." Neurocomputing, 2015, 165(C):38-45.

[37] Cichocki A, Mandic D, Lathauwer L D, et al, "Tensor Decompositions for Signal Processing Applications: From two-way to multiway component analysis." IEEE Signal Processing Magazine, 2014, 32(2):145-163.

[38] Phan A H, Cichocki A, "Tensor decompositions for feature extraction and classification of high dimensional datasets." Nonlinear Theory & Its Applications Ieice, 2010, 1(1):37-68.

[39] Bhaskara A, Charikar M, Vijayaraghavan A, "Uniqueness of Tensor Decompositions with Applications to Polynomial Identifiability." Journal of Machine Learning Research, 2013, 35:742-778.

[40] Zhang Z Y, Li T, Ding C, "Non-negative Tri-factor tensor decomposition with applications." Knowledge & Information Systems, 2013, 34(2):243-265.

**Wei Wang** received his Ph.D. degree in Tianjin University, he is currently Professor in College of Electronic and Communication Engineering, Tianjin Normal University, Tianjin, China.

His main research directions involve Compressive Sensing, radar signal processing, deep learning and Multimodal data fusion and so on.

**Min Zhang** is currently working toward the Graduate degree in College of Electronic and Communication Engineering, Tianjin Normal University, Tianjin, China.

His research interests include heterogeneous data fusion and processing, deep learning, tensor space and big data mining.

**Li Zhang** is currently working toward the Graduate degree in College of Electronic and Communication Engineering, Tianjin Normal University, Tianjin, China.

His research interests include high dimensional small sample, deep learning, tensor space and migration learning.